Combined DØ and CDF Upper Limits on Standard-Model Higgs-Boson Production

The TEVNPH Working Group*

for the DØ and CDF Collaborations

We combine results of CDF and DØ searches for a Standard-Model Higgs boson (H) in data from $p\bar{p}$ collisions at the Fermilab Tevatron with $\sqrt{s} = 1.96$ TeV. With 260-950 pb^{-1} collected at DØ ,and 360-1000 pb^{-1} collected at CDF, the 95% CL upper limits are a factor of 10.4(3.8) higher than the expected cross section for m_H =115(160) GeV/c^2. This result extends significantly the individual limits of each experiment.

I. INTRODUCTION

Because the mechanism for electroweak symmetry breaking has yet to be confirmed, the search for a Standard-Model (SM) Higgs boson represents a significant issue in Fermilab's Tevatron physics program. Both DØ and CDF have recently reported searches for Higgs bosons that combined different final states and production modes[1, 2].

In this note, we combine results of all such searches from CDF and DØ for $p\bar{p}$ collisions at $sqrts = 1.96$ TeV. These searches are for SM Higgs bosons produced in association with vector bosons ($p\bar{p} \rightarrow W/ZH \rightarrow \ell\nu b\bar{b}/\nu\bar{\nu}b\bar{b}/\ell^+\ell^-b\bar{b}$ or $p\bar{p} \rightarrow WH \rightarrow WW^+W^-$) or singly through gluon-gluon fusion ($p\bar{p} \rightarrow H \rightarrow W^+W^-$). The results are for data corresponding to integrated luminosities ranging from 360-1000 pb^{-1} at CDF and 260-950 pb^{-1} at DØ . The searches are separated into sixteen final states, referred to as analyses in the following. To simplify combination of signals, the analyses are separated into sixteen mutually exclusive final states. Selection procedures for each analysis are detailed in each of the experiment's reports[1, 2], and briefly described below.

II. ACCEPTANCE, BACKGROUNDS, AND LUMINOSITY

Selections are similar for the corresponding CDF and DØ analyses. For the case of $WH \rightarrow \ell\nu b\bar{b}$, an isolated lepton (electron or muon) and at least two jets are required, with one or more jets tagged as originating from b-quarks. Two orthogonal tagging criteria are defined, one being an exclusive single-tag (ST) and the other a double-tag(DT) selection. These events must also display a significant imbalance of momentum in the plane transverse to the beam axis (referred to as missing energy or $\not{E}_T$). Events with additional isolated leptons are vetoed. For the $ZH \rightarrow \nu\bar{\nu}b\bar{b}$ analyses, the selection is similar, except all events with isolated leptons are vetoed and stronger multijet background suppression techniques are applied. As there is a sizable amount of $WH \rightarrow \ell\nu b\bar{b}$ signal that can mimic the $ZH \rightarrow \nu\bar{\nu}b\bar{b}$ final state when the lepton is undetected, the DØ analyses include this as a separate search, referred to as $WH \rightarrow \ell\nu b\bar{b}$. CDF includes this as part of the acceptance of the $ZH \rightarrow \nu\bar{\nu}b\bar{b}$ search. In the $WH \rightarrow \ell\nu b\bar{b}$ and $ZH \rightarrow \nu\bar{\nu}b\bar{b}$ analyses, the final variable used for setting a cross section limit is the dijet invariant mass. The $ZH \rightarrow \ell^+\ell^-b\bar{b}$ analyses require two isolated leptons and two jets, wherein the CDF analysis requires at least one of the jets to be b-tagged while the DØ analysis uses only events with two b-tags. For the DØ analysis the dijet invariant mass is used for setting limits while CDF uses the output of a 2-dimensional Neural Network to discriminate between signal and background. For the $H \rightarrow W^+W^-$ analyses, a large $\not{E}_T$ and two opposite-signed, isolated leptons (electrons or muons) are selected, defining three final states (e^+e^-, $e^\pm\mu^\mp$, and $\mu^+\mu^-$). The presence of neutrinos in the final state prevents the direct reconstruction of the Higgs mass, and the final variable used is the difference in φ between the two final-state leptons. The DØ experiment also contributes three $WH \rightarrow WW^+W^-$ analyses, where the associated W boson and the same-charged W boson from the Higgs decay semi-leptonically, thereby defining six final states containing all decays of the

TABLE I: The luminosity, expected signal, expected background, and observed data for the CDF analyses. Also included is the Higgs mass for which each set of numbers are derived. For the $ZH \to \nu\bar{\nu}b\bar{b}$ analysis the signal events are given separately for WH and ZH events. The numbers of expected events are determined for $0 \leq m_{jj} \leq 200$ GeV/c^2 for $H \to b\bar{b}$ analyses, and $0 \leq \Delta\varphi(\ell_1, \ell_2) \leq \pi$ for $H \to W^+W^-$ analyses.

	$WH \to \ell\nu b\bar{b}$ DT(ST)	$ZH \to \nu\bar{\nu}b\bar{b}$ DT(ST)	$ZH \to \ell^+\ell^- b\bar{b}$	$H \to W^+W^- \to \ell^\pm\nu\ell^\mp\nu$
Luminosity (pb^{-1})	1000	1000	1000	360
Expected Signal (evts)	0.50 (1.47)	0.25+0.22 (0.77+0.64)	0.64	0.84
Expected Background (evts)	40.2 (366.3)	19.6 (309.9)	103.7	13.8
Data (evts)	36 (390)	24 (333)	104	18
m_H (GeV/c^2)	115	115	120	160
Reference	[12]	[13]	[14]	[15]

TABLE II: The luminosity, expected signal, expected background, and observed data for the DØ $H \to b\bar{b}$ analyses. The number of expected signal, background, and data are determined for $0 \leq m_{jj} \leq 200$ GeV/c^2.

	$WH \to e\nu b\bar{b}$ DT(ST)	$WH \to \mu\nu b\bar{b}$ DT(ST)	$WH \to \ell\nu b\bar{b}$ DT(ST)	$ZH \to \nu\bar{\nu}b\bar{b}$ DT(ST)	$ZH \to \ell^+\ell^- b\bar{b}$
Luminosity (pb^{-1})	371	385	260	260	320-389
Expected Signal (evt)	0.19 (0.22)	0.11 (0.12)	0.18 (0.20)	0.24 (0.26)	0.11
Expected Background (evts)	14.6 (58.3)	10.2 (46.8)	25.2 (87.3)	25.2 (87.3)	11.0
Data (evts)	14 (57)	8 (48)	23 (98)	23 (98)	14
m_H (GeV/c^2)	115	115	115	115	115
Reference	[16]	[16]	[17]	[17]	[18]

third W boson (of opposite charge). In this case of this analysis, the final variable is a likelihood discriminant formed from several topological variables.

All Higgs signals are simulated using PYTHIA v6.202[3], using CTEQ5L[4] leading order parton distribution functions. The signal cross sections are normalized to next-to-next-to-leading order calculations[5, 6], and branching ratios from HDECAY[7]. For both CDF and DØ , events from multijet (instrumental) backgrounds ("QCD production") are measured in data, but with different methods. For CDF, inherent backgrounds from other SM processes were generated using PYTHIA, ALPGEN[8], and HERWIG[9] programs. For DØ , inherent backgrounds were generated using PYTHIA, ALPGEN, and COMPHEP[10], with PYTHIA providing parton-showering and hadronization for all the generators. Background processes were normalized using either experimental data or next-to-leading order calculations from MCFM[11].

Values of integrated luminosity, and expected signal, expected background, and observed events are given in Table I for CDF analyses and Tables II-III for DØ analyses. The numbers of events are integrated in the range $0 \leq m_{jj} \leq 200$ GeV/c^2 for $H \to b\bar{b}$ analyses, $0 \leq \Delta\varphi(\ell_1, \ell_2) \leq \pi$ for $H \to W^+W^-$ analyses, and $0 \leq Discrim \leq 1$ for the $WH \to WW^+W^-$ analyses. The tables also include the value of the Higgs mass for which each set of numbers is derived.

TABLE III: The luminosity, expected signal, expected background, and observed data for the DØ $WH \to WW^+W^-$ analyses. The number of expected signal, background, and data are determined for $0 \leq \Delta\varphi(\ell_1, \ell_2) \leq \pi$.

	$WW^+W^- \to e^\pm\nu e^\pm\nu$	$WW^+W^- \to e^\pm\nu\mu^\pm\nu$	$WW^+W^- \to \mu^\pm\nu\mu^\pm\nu$
Luminosity (pb^{-1})	384	368	363
Expected Signal (evts)	0.043	0.101	0.066
Expected Background (evts)	15.4	7.0	12.5
Data (evts)	15	7	12
m_H (GeV/c^2)	155	155	155
Reference	[19]	[19]	[19]

TABLE IV: The luminosity, expected signal, expected background, and observed data for the DØ $H \rightarrow W^+W^-$ analyses. The number of expected signal, background, and data are determined for $0 \leq \Delta\varphi(\ell_1, \ell_2) \leq \pi$.

	$H \rightarrow W^+W^- \rightarrow e^+\nu e^-\nu$	$H \rightarrow W^+W^- \rightarrow e^\pm\nu\mu^\mp\nu$	$H \rightarrow W^+W^- \rightarrow \mu^+\nu\mu^-\nu$
Luminosity (pb^{-1})	950	950	930
Expected Signal (evts)	0.64	1.50	0.54
Expected Background (evts)	11.4	28.1	10.5
Data (evts)	11	18	10
m_H (GeV/c^2)	160	160	160
Reference	[20]	[20]	[21]

III.   COMBINATION PROCEDURES

To gain confidence that the final result does not depend on the details of the statistical formulation, we combine all separate results using both a Bayesian and a Frequentist approach. In both methods, distributions in the final variables are binned according to their experimental resolution, rather than as single integrated values. Systematic uncertainties enter as uncertainties on the expected number of signal and background events in each analysis. Both methods use likelihood calculations based upon Poisson probabilities.

A.   Frequentist Method

The Frequentist technique relies on the CL_s method, using a log-likelihood ratio (LLR) as test statistic[1], as given by:

$$LLR_n = 2\sum_{i=1}^{N} \left(s_i - n_i \text{Log}(1 + s_i/b_i) \right) \tag{1}$$

where n denotes the hypothesis being tested (*e.g.*, background-only or observed data) and the sum runs over the number of bins (and/or analyses) being combined. The value of CL_s is then defined as the normalization of the signal+background hypothesis (CL_{s+b}) by the background-only hypothesis (CL_b). This construction reduces the ambiguity of "unphysical" results (*e.g.*, negative cross section limits) and separates properties of the estimator from that of the quantity being probed.

B.   Bayesian Method

Because there is no information on the production cross section for the Higgs, the Bayesian technique[2] assigns a flat prior for the total number of Higgs events. For a given Higgs mass, the combined likelihood is a product of the likelihoods in the individual channels, each of which is a product over histogram bins:

$$\mathcal{L}(R, \vec{s}, \vec{b}|\vec{n}) = \prod_{i=1}^{N_C} \prod_{j=1}^{Nbins} \mu_{ij}^{n_{ij}} e^{-\mu_{ij}}/n_{ij}! \tag{2}$$

where the first product is over the number of channels (N_C), and the second product is over histogram bins containing n_{ij} observed events, either in dijet mass for WH and ZH, in $\Delta\varphi$ of two leptons for $H \rightarrow W^+W^-$, or in the likelihood discriminant for $WH \rightarrow WW^+W^-$ events. The parameters that contribute to the expected bin contents are $\mu_{ij} = R \times s_{ij} + b_{ij}$ for the channel i and the histogram bin j. The posterior density function is then integrated over all parameters (including correlations) except for R, and a 95% credibility level upper limit on R is estimated by calculating the value of R that corresponds to 95% of the area of the resulting distribution.

TABLE V: The breakdown of systematic uncertainties for each individual CDF analysis. All positive-signed uncertainties within a group are considered 100% correlated across channels. Values with negative signs are considered uncorrelated.

Source	$WH \to \ell\nu b\bar{b}$ ST	$WH \to \ell\nu b\bar{b}$ DT	$ZH \to \nu\bar{\nu}b\bar{b}$ ST	$ZH \to \nu\bar{\nu}b\bar{b}$ DT	$ZH \to \ell^+\ell^- b\bar{b}$	$H \to W^+W^-$
Luminosity (%)	6.0	6.0	6.0	6.0	6.0	6.0
b-Tag Scale Factor (%)	5.3	16.0	8.0	16.0	8.0	n/a
Lepton Identification (%)	2.0	2.0	2.0	2.0	1.4	3.0
Jet Energy Scale (%)	3.0	3.0	6.0	(1.0-20.0)	(1.6-20.0)	1.0
I(S)R+PDF (%)	4.0	10.0	4.0	5.0	2.0	5.0
Trigger (%)	0.0	0.0	3.0	3.0	0.0	0.0
$Z + h.f.$ Shape (%)	n/a	n/a	n/a	n/a	-20	n/a
Backgrounds						
W/Z+HF(I) (%)	33.0	34.0	12.0	12.0	40.0	n/a
W+HF(II) (%)	0	0	-10.0	-42.0	0	n/a
Z+HF(II) (%)	0	0	-6.0	-19.0	0	n/a
Mistag (%)	22.0	15.0	17.0	17.0	17.0	n/a
Top I (%)	13.5	20.0	12.0	12.0	20.0	n/a
Top II (%)	n/a	n/a	-2.0	-3.0	n/a	n/a
QCD (%)	17.0	20.0	-10.0	-44.0	-50.0	n/a
Diboson I (%)	16.0	25.0	12.0	12.0	20.0	11.0
Diboson I (%)	n/a	n/a	-5.0	-10.0	n/a	n/a
Others (%)	n/a	n/a	n/a	n/a	n/a	-(12.0-18.0)

C. Systematic Uncertainties

Systematic uncertainties on background are generally several times larger than the expected signal, and are therefor important in the limit calculation. Each systematic uncertainty is folded into the signal and background expectations assuming Gaussian distributions. The Gaussian values are sampled once for each Poisson Monte Carlo (MC) trial (pseudo-experiment). Correlations among systematic sources are carried through in the calculation. Systematic uncertainties differ between experiments and analyses, both for signal and background sources. Detailed discussions of these issues can be found in the individual analysis notes[1, 2]. Here we will consider only the largest contributions and correlations among and within the two experiments.

1. Correlated Systematics

The uncertainty on the measurement of the integrated luminosity is 6% (CDF) and 6.5% (DØ). Of this value, 4% arises from the uncertainty on the inelastic $p\bar{p}$ scattering cross section, which is correlated between CDF and DØ . The uncertainty on the production rates for top-quark processes ($t\bar{t}$ and single-top) and electroweak processes (WW, WZ, and ZZ) are also taken as correlated between the two experiments. As the methods of measuring the multijet (QCD) backgrounds differ between CDF and DØ , there is no correlation assumed for this uncertainty.

2. CDF Systematics

The dominant systematic uncertainties for the CDF analyses are shown in Table V. For $H \to b\bar{b}$, the largest uncertainties on signal arise from the b-tagging scale factor (5.3-16%), jet energy scale (1-20%), and MC modeling (2-10%). For $H \to W^+W^-$, the largest contributing uncertainty comes from MC modeling (5%). For inherent backgrounds, the uncertainties on the expected rates range from 11-40% (depending on background). Because the largest background contributions are measured using data, these uncertainties are treated as uncorrelated for the $H \to b\bar{b}$ channels. For the $H \to W^+W^-$ channel, the luminosity uncertainty is taken to be correlated between signal and background. The differences between treating the remaining uncertainties to be correlated or uncorrelated is less than 5%.

TABLE VI: List of leading correlated systematic uncertainties for the DØ analyses. The values for the systematic uncertainties are the same for the $ZH \to \nu\bar{\nu}b\bar{b}$ and $WH \to \ell\nu b\bar{b}$ channels. All uncertainties with a common origin are considered 100% correlated across channels. The correlated systematic uncertainty on the background cross section (σ) is itself subdivided according to the different background processes in each analysis.

Source	$WH \to e\nu b\bar{b}$ DT(ST)	$WH \to \mu\nu b\bar{b}$ DT(ST)	$H \to W^+W^-, WH \to WW^+W^-$
Luminosity (%)	6.5	6.5	6.5
Jet Energy Scale (%)	4.0	5.0	3.0
Jet ID (%)	6.8	6.8	0
Electron ID (%)	6.6	0	2.3
Muon ID (%)	0	4.9	7.7
b-Jet Tagging (%)	8.5(5.0)	8.5(5.0)	0
Background σ (%)	6.0-19.0	6.0-19.0	6.0-19.0

Source	$ZH \to \nu\bar{\nu}b\bar{b}$ DT(ST)	$ZH \to e^+e^- b\bar{b}$	$ZH \to \mu^+\mu^- b\bar{b}$
Luminosity (%)	6.5	6.5	6.5
Jet Energy Scale (%)	6.0	7.0	2.0
Jet ID (%)	7.1	7.0	5.0
Electron ID (%)	0	8.0	0
Muon ID (%)	0	0	12.0
b-Jet Tagging (%)	9.6(6.7)	12.0	22.0
Background σ (%)	6.0-19.0	6.0-19.0	6.0-19.0

3. DØ Systematics

The dominant systematic uncertainties for DØ analyses are shown in Table VI. The $H \to b\bar{b}$ analyses have an uncertainty on the b-tagging rate of 5-7% per tagged jet. These analyses also have an uncertainty on the jet measurement and acceptance of 6-9% (jet identification or jet ID, energy scale, and jet smearing). For the $H \to W^+W^-$ and $WH \to WW^+W^-$, the largest uncertainties are associated with lepton measurement and acceptance. These values range from 3-6% depending on the final state. The largest contributing factor to all analyses is the uncertainty on the cross sections for inherent background at 6-15%. These systematics are assumed to apply to both signal and background processes. All systematic uncertainties arising from the same source are taken to be correlated between signal and background, as detailed in Table VI.

IV. COMBINED RESULTS

Using the combination procedures outlined above, we extract limits on SM Higgs boson production $\sigma \times BR*(H \to X)$ in $p\bar{p}$ collisions at $\sqrt{s} = 1.96$ TeV. Figure 1 displays the log-likelihood ratio distributions for the combined analyses as a function of m_H. Included are the results for the background-only hypothesis (LLR$_b$), the signal+background hypothesis (LLR$_{s+b}$), and the observed data (LLR$_{obs}$). The shaded bands represent the 1 and 2 standard deviation (σ) departures for LLR$_b$. These distributions can be interpreted as follows:

- The separation between LLR$_b$ and LLR$_{s+b}$ provides a measure of the overall power of the search. This is the ability of the analysis to discriminate between the $s + b$ and $b-$only hypotheses.

- The width of the LLR$_b$ distribution (shown here as 1 and 2 standard deviation bands) provides an estimate of how sensitive the analysis is to a signal-like fluctuation in data, taking account of the presence of systematic uncertainties. For example, when a 1-σ background fluctuation is large compared to the signal expectation, the analysis sensitivity is thereby limited.

- The value of LLR$_{obs}$ relative to LLR$_{s+b}$ and LLR$_b$ indicates whether the data distribution appears to be more signal-like or background-like. As noted above, the significance of any departures of LLR$_{obs}$ from LLR$_b$ can be evaluated by the width of the LLR$_b$ distribution.

To facilitate model transparency and to accommodate analyses with different degrees of sensitivity, we present our results in terms of the ratio of limits set to the SM cross sections as a function of Higgs mass. A value of < 1 would indicate a Higgs mass excluded at 95% CL. The expected and observed 95% upper limit ratios to the SM cross section

for the combined CDF and DØ analyses are shown in Figure 2. The observed and expected limit ratios are listed for selected Higgs masses in Table VII, with observed(expected) values of 10.4(7.6) at $m_H = 115$ GeV/c^2 and 3.8(5.0) at $m_H = 160$ GeV/c^2.

These results represent an improvement in search sensitivity over those obtained for individual experiments, which have set observed(expected) limit ratios of 16.3(16.7) for DØ and 12.8(9.1) for CDF at $m_H = 115$ GeV/c^2 and of 4.3(5.9) for DØ and 11.4(10.2) for CDF at $m_H = 160$ GeV/c^2.

---

[1] DØ Collaboration, Conference Note 5056, "Limits on Standard Model Higgs Boson Production"
[2] CDF Collaboration, "Combined Upper Limit on Standard Model Higgs Boson Production at CDF for Summer 2006," CDF/ANAL/EXOTIC/PUBLIC/8403
[3] T. Sjostrand, L. Lonnblad and S. Mrenna, "PYTHIA 6.2: Physics and manual," [arXiv:hep-ph/0108264]
[4] H. L. Lai *et al.*, *Improved Parton Distributions from Global Analysis of Recent Deep Inelastic Scattering and Inclusive Jet Data*, Phys. Rev D **55** (1997) 1280
[5] S. Catani, D. de Florian, M. Grazzini and P. Nason, "Soft-gluon resummation for Higgs boson production at hadron colliders," JHEP **0307**, 028 (2003), [arXiv:hep-ph/0306211]
[6] K. A. Assamagan *et al.* [Higgs Working Group Collaboration], "The Higgs working group: Summary report 2003," [arXiv:hep-ph/0406152]
[7] A. Djouadi, J. Kalinowski and M. Spira, "HDECAY: A program for Higgs boson decays in the standard model and its supersymmetric extension," Comput. Phys. Commun. **108**, 56 (1998) [arXiv:hep-ph/9704448]
[8] M. L. Mangano, M. Moretti, F. Piccinini, R. Pittau and A. D. Polosa, "ALPGEN, a generator for hard multiparton processes in hadronic collisions," JHEP **0307**, 001 (2003) [arXiv:hep-ph/0206293]
[9] G. Corcella *et al.*, "HERWIG 6: An event generator for hadron emission reactions with interfering gluons (including supersymmetric processes)," JHEP **0101**, 010 (2001) [arXiv:hep-ph/0011363]
[10] A. Pukhov *et al.*, "CompHEP: A package for evaluation of Feynman diagrams and integration over multi-particle phase space. User's manual for version 33," [arXiv:hep-ph/9908288]
[11] J. Campbell and R. K. Ellis, "Next-to-leading order corrections to W + 2jet and Z + 2jet production at hadron colliders," Phys. Rev. D **65**, 113007 (2002), [arXiv:hep-ph/0202176]
[12] CDF Collaboration, "Search for Higgs Boson Production in Association with W Boson with 1 fb^{-1}," CDF/ANAL/EXOTIC/PUBLIC/8390
[13] CDF 1 fb^{-1} ZH result.
[14] CDF 1 fb^{-1} ZH result in dilepton channel.
[15] CDF Collaboration, "Search for the Standard Model Higgs Boson in the $gg \to H \to WW^*$ Dilepton Channel with 360 pb^{-1}," CDF/ANAL/EXOTIC/PUBLIC/7893
[16] DØ Collaboration, "Search for WH Production at $\sqrt{s} = 1.96$ TeV," DØ Conference Note 5054
[17] DØ Collaboration, "A Search for the Standard Mondel Higgs boson using the $ZH \to \nu\bar{\nu}b\bar{b}$ channel in $p\bar{p}$ Collisions at $\sqrt{s} = 1.96$ TeV," submitted to Phys. Rev. Lett., [arXiv:hep-ex/0607022]
[18] DØ Collaboration, "A Search for $ZH \to \ell^+\ell^-b\bar{b}$ Production at DØ in $p\bar{p}$ Collisions at $\sqrt{s} = 1.96$ TeV," DØ Conference Note 5186
[19] DØ Collaboration, "Search for associated Higgs boson production $WH \to WWW^* \to \ell^\pm\nu\ell'^\pm\nu' + X$ in $p\bar{p}$ collisions at $\sqrt{s} = 1.96$ TeV," submitted to Phys. Rev. Lett., [arXiv:hep-ex/0607032]
[20] DØ Collaboration, "Search for the Higgs boson in $H \to WW^* \to l^+l^-(ee, e\mu)$ decays with 950 pb^{-1} at DØ in Run II," DØ Conference Note 5063
[21] DØ Collaboration, "Search for the Higgs boson in $H \to WW^* \to \mu\mu$ decays with 930 pb^{-1} at DØ in Run II," DØ Conference Note 5194

TABLE VII: Expected and observed 95% CL cross section ratios for the combined CDF and DØ analyses.

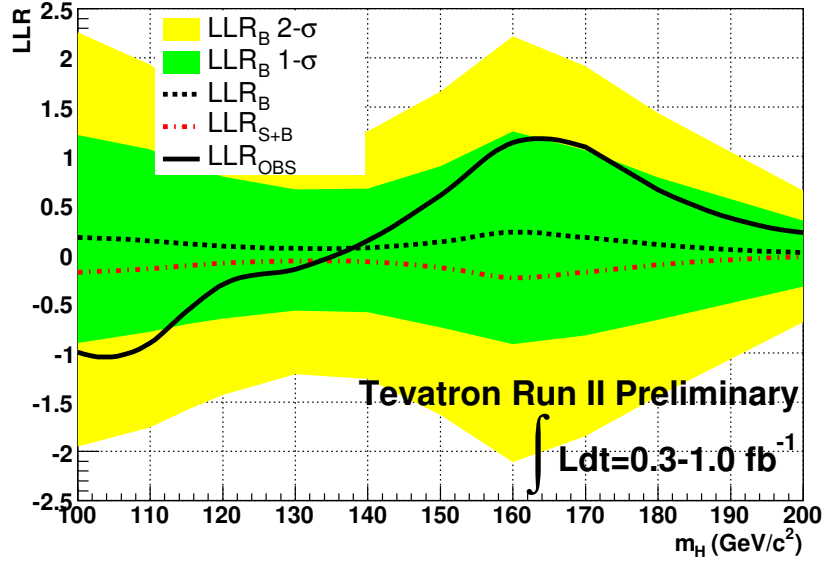|	100 GeV/c²	115 GeV/c²	120 GeV/c²	140 GeV/c²	160 GeV/c²	180 GeV/c²	200 GeV/c²
Expected	6.2	7.6	8.7	9.3	5.0	7.5	15.5
Observed	8.5	10.4	11.1	8.8	3.8	6.1	12.3

FIG. 1: Log-likelihood ratio distribution for the combined CDF and DØ analyses. Shown in the plot are the LLR_b (background-only hypothesis), LLR_{s+b} (signal+background hypothesis), LLR_{obs} (observed LLR value), and the 1-σ and 2-σ bands for the LLR_b distribution.
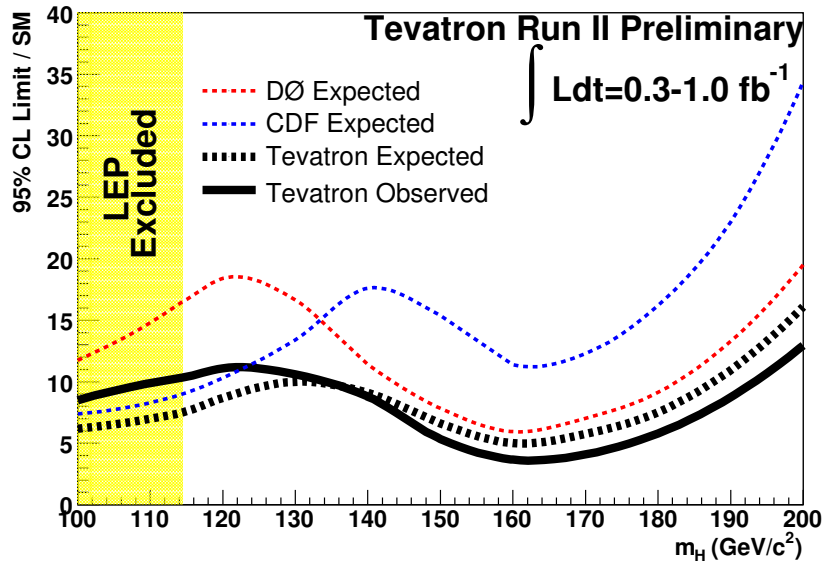
FIG. 2: Expected and observed 95% CL cross section ratios for the combined CDF and DØ analyses. Also shown are the expected 95% CL ratios for the CDF and DØ experiments alone.